

## PHYSICAL MODELLING OF ALUMINUM MELT DEGASSING IN LOW-PRESSURE DIE CASTING CONDITIONS

<sup>1</sup>Ladislav SOCHA, <sup>2,3</sup>Tomáš PRÁŠIL, <sup>1</sup>Karel GRYC, <sup>1</sup>Jana SVIŽELOVÁ, <sup>3</sup>Petr NOVÁČEK

<sup>1</sup>*Institute of Technology and Business in České Budějovice, České Budějovice, Czech Republic, EU, [socha@mail.vstecb.cz](mailto:socha@mail.vstecb.cz), [gryc@mail.vstecb.cz](mailto:gryc@mail.vstecb.cz), [svizelova@mail.vstecb.cz](mailto:svizelova@mail.vstecb.cz)*

<sup>2</sup>*University of West Bohemia, Plzeň, Czech Republic, EU, [tprasil@kmm.zcu.cz](mailto:tprasil@kmm.zcu.cz)*

<sup>3</sup>*MOTOR JIKOV Slévárna a.s., Die-casting Division, České Budějovice, Czech Republic, EU, [TPrasil@mjgroup.cz](mailto:TPrasil@mjgroup.cz), [PNovacek@mjsl.cz](mailto:PNovacek@mjsl.cz)*

<https://doi.org/10.37904/metal.2022.4511>

### Abstract

This paper deals with approximate physical modelling of aluminum melt degassing, performed under low-pressure die casting conditions of aluminum castings. The modelling took place on an aquatic physical model on a 1:1 scale to the operating conditions, constructed in the laboratories of ITB in ČB. Tested parameters were defined based on operating conditions (rotation speed and inert gas flow). Various combinations of these parameters created 20 tested variants, including the current set of parameters used in operating conditions. The effects of the tested parameters were determined using the results of measurement. Increasing the rotation speed and the inert gas flow accelerates gas removal from the model liquid. It will be possible to further use this knowledge in refining technology optimization in the low-pressure aluminum die casting.

**Keywords:** Physical modelling, aluminum, refinement process, FDU, low pressure die casting

### 1. INTRODUCTION

Aluminum alloys contain a number of impurities with negative impact on aluminum castings properties. Regarding the relevant phases; we can mention, in particular, hydrogen and non-metallic inclusions. Humidity contained in batch raw materials and in other materials, which come into contact with the melt, is usually the hydrogen source [1,2]. In order to remove the impurities, a refinement process is included in the aluminum castings production technology. Refining the aluminum melt on a FDU device (Foundry Degassing Unit) is a standard part of the aluminum castings production. The FDU technology principle lies in blowing of inert gas into which diffuses hydrogen from an aluminum melt [2]. The inert gas is supplied via a rotor which divides it into tiny bubbles. Simultaneously, undesirable inclusions are removed by refining salts. The aluminum melt refinement process on a FDU device is shown on **Figure 1**.

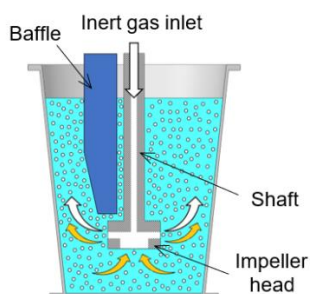


**Figure 1** Principle of the FDU device [3]



**Figure 2** FDU device for low-pressure die casting

There exist many studies dealing with the aluminum melt issue [4-13]. However, the relevant issue is still topical, since every company producing aluminum castings is characterised by specific conditions and the research specialization has to be adjusted to the relevant conditions.

The study is a part of a research project that deals with the refining technologies research and development, the purpose of which is to increase the quality of aluminum alloys intended for heavy duty castings, manufactured by the MOTOR JIKOV Slévárna a.s. die casting foundry. The project subject is development and innovation of production technology and aluminum alloys refinement [14,15]. The aluminum melt refinement is realized through two FDU devices for high-pressure and low-pressure casting. The FDU device for low-pressure casting is shown on **Figure 2**. Operating experiments and physical modelling together with operating verification are used for complex production technologies development.

The presented paper focuses on physical modelling of refinement on a FDU device at low-pressure casting conditions. Its goal is comparison of aluminum melt refinement on a FDU device at various settings of the operating conditions. The research took place in the ITB in ČB, Environmental research centre laboratories, using an aquatic physical model. The physical modelling purpose was simulation of the relevant process to such an extent when it would be possible to assess its intensity and then apply the obtained knowledge in operating conditions. Experiments with various settings of the selected parameters which also included the standard variant used in operating conditions were realized for this purpose. An optimized combination of the studied parameters for testing in operating conditions will be designed on the basis of the results obtained.

## 2. DESCRIPTION OF PHYSICAL MODEL AND EXPERIMENTAL METHODOLOGY

An aquatic physical model of a refinement facility shown on **Figure 3** has been constructed for the purposes of an aluminum alloy degassing physical modelling. The physical model was constructed according to the FDU facility used by the MOTOR JIKOV Slévárna a.s. The basic components of the system are a Plexiglas vessel (a refining ladle model), a graphite rotor, a baffle and optical probes for measuring of oxygen concentration in water. The rotor is driven by an electrical motor with speed control. In order to maintain the geometrical similarity of the FDU facility and the model, the model vessel was manufactured on the 1:1 scale to the refining ladle.

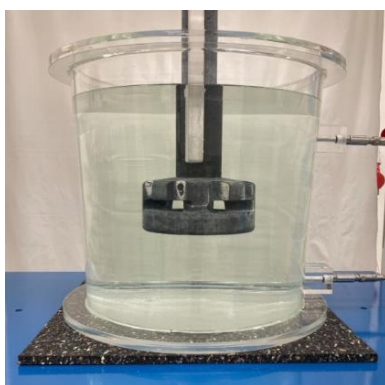


**Figure 3** Illustration of a physical model and base dimensions of the model assembly

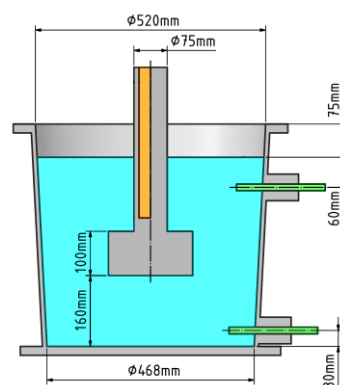


**Figure 4** Impeller design

The physical modelling principle was capturing of the melt degassing intensity and analysing of the harmful gas content decrease at various parameters change at laboratory conditions. It was necessary to decide on an appropriate methodology for this purpose, which would ensure maintaining of the FDU facility dynamical similarity to the model. Therefore, the alloy melt was replaced by water and the removed hydrogen by oxygen. For illustration, basic properties of the aluminum alloy and of the model media are given in **Table 1**.

**Table 1** Properties of molten aluminum and model media

Parameter	Aluminum	Water	Oxygen
Temperature (°C)	750	20	20
Density (kg·m <sup>-3</sup> )	2.345	998.2	1.299
Dynamic viscosity (kg·m <sup>-1</sup> ·s <sup>-1</sup> )	1.200·10 <sup>-3</sup>	1.003·10 <sup>-3</sup>	0.019·10 <sup>-3</sup>
Kinematic viscosity (m <sup>2</sup> ·s <sup>-1</sup> )	0.51·10 <sup>-6</sup>	1.01·10 <sup>-6</sup>	14.77·10 <sup>-6</sup>

**Table 2** specifies the operating conditions of aluminum melt refinement which served as a basis for determination of physical modelling conditions for the examined rotor type. The parameters proper and individual experiments conditions on the FDU device physical model have been designed in cooperation with the MOTOR JIKOV Slévárna a.s. die casting foundry technologists. Below are specified the basic parameters taken into consideration at defining the modelled variants: rotor type, working height, baffles number, speed (rpm), inert gas flow rate (Ar). Based on the relevant conditions laboratory experiments on a physical model were defined and realized.

**Table 2** Comparison of operating conditions with the physical model

Parameter	Operating conditions	Physical model
Working height of impeller (mm)	160	160
Number of baffles (pc)	1	1
Refinement time (s)	180	180
Rotation frequency (rpm)	350	325 to 400
Inert gas type (-)	Nitrogen	Argon
Inert gas flow rate (Nl·min <sup>-1</sup> )	17	13 to 19

Within the presented research, attention was focused on specification of individual process parameters influence on the intensity of oxygen removal from water. The rotor shown on **Figure 4**, which is standardly used in operating conditions of aluminum alloys low-pressure casting, has been selected for the relevant purpose. The rotor efficiency was verified at various setting of the parameters; therefore, experiments variants with various rotation frequency and various inert gas flow were defined. In order to verify the relevant parameters influence on the degasification intensity, 20 variants of experiments have been realized for every rotor type. Their parameters are presented in **Table 3**.

**Table 3** Settings of modelled variants (working height: 160 mm, baffles: 1 pc)

Rotation frequency (rpm)	300					325					350					375				
Argon flow rate (Nl·min <sup>-1</sup> )	13	15	17	19	21	13	15	17	19	21	13	15	17	19	21	13	15	17	19	21

### 3. RESULTS AND DISCUSSION

For the purpose of illustration regarding the course, efficiency and characters of events, **Figure 5** gives examples of concentration curves measured on the FDU device physical model at the speed and gas flow rate change according to the designed variants, specified in **Table 3**. The curves show clearly the degasification course and the total refinement time. The total refinement time has been specified for the physical modelling purposes as the time which is required for reaching the concentration of 0.5 ppm of oxygen in water.

Based on the data measured, it can be stated in general that with the increasing speed (rpm), the process of oxygen concentration decrease in water accelerates. A similar conclusion can be noted also with regard to the

argon flow rate. With the increasing argon flow rate, the oxygen is removed from water faster. However, there exist exceptions in the form of variants with 375 rpm. The graphs on **Figure 5** show clearly significant extension of the total refinement time, since at a certain phase of the process when the oxygen level in water decreased under ca 0.6 ppm, the speed of oxygen removal from water decreased. The relevant phenomenon occurrence will be verified in operating conditions in the next stages of the research.

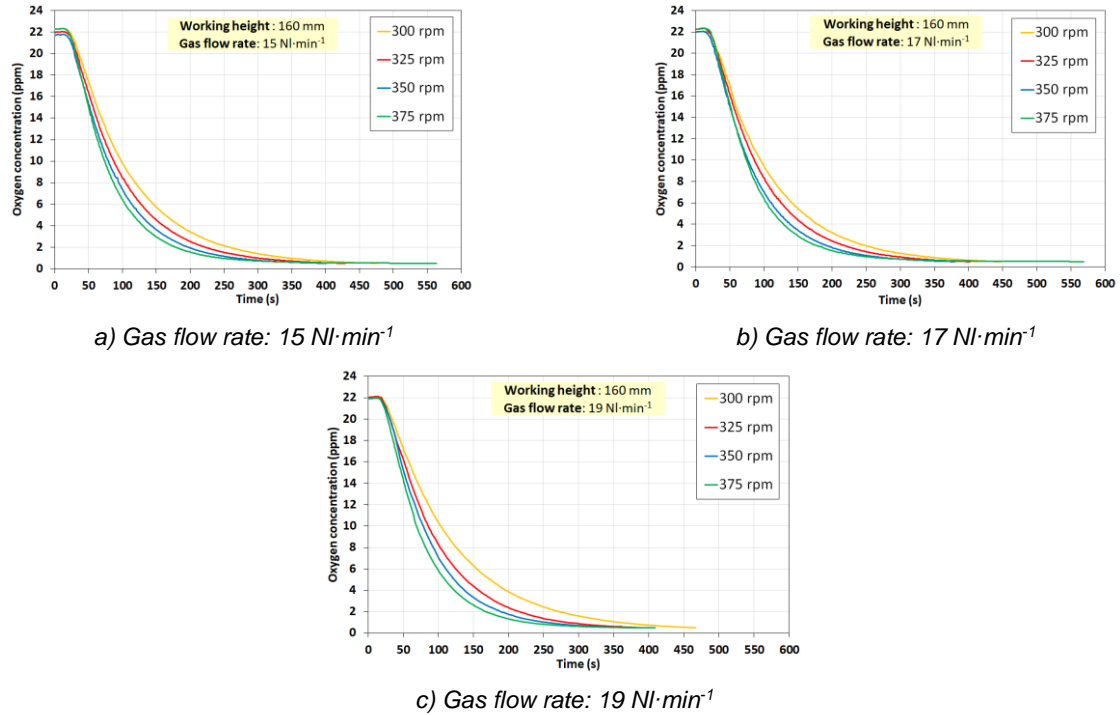


**Figure 5** Oxygen concentration change at various argon flow rate and various speed

Besides graphic processing of the oxygen concentration decrease course during refinement by inert gas supplied via a rotor, video sequences and photographs were taken within the experiment course, documenting liquid flowing and distribution of developing bubbles of blown argon for individual variants.

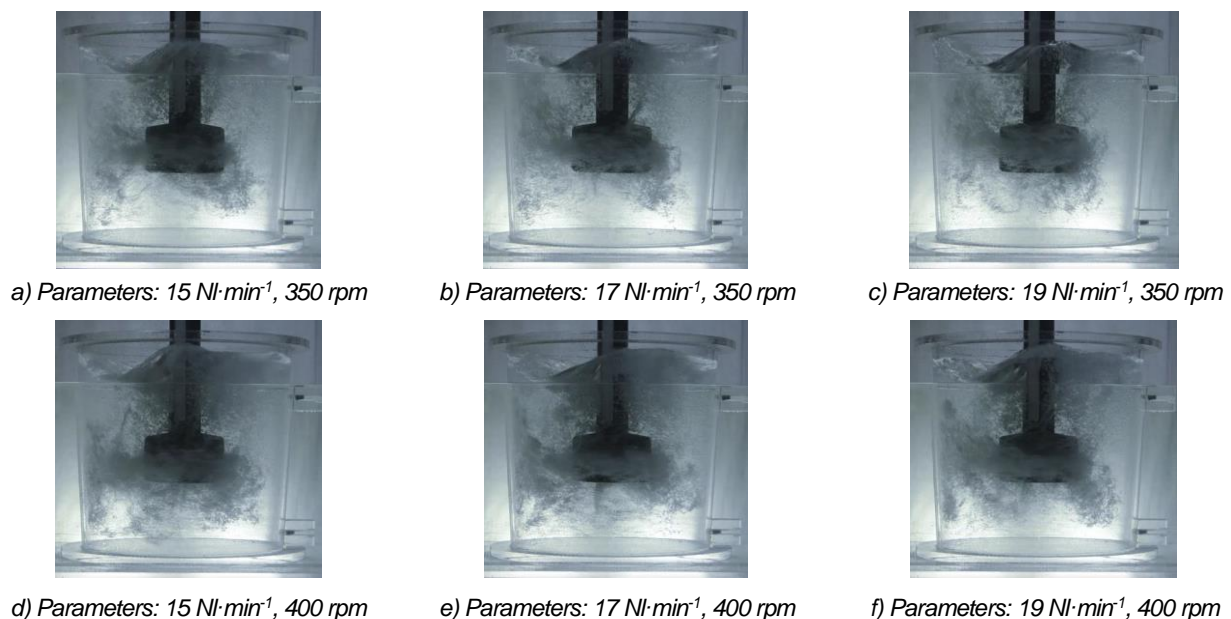


**Figure 6** Visualization of internal flow and distribution of argon bubbles

**Figure 6** shows examples of photographs depicting the character of internal flow at the change of speed and argon flow.

General comparison and evaluation of all measured variants was carried out on the basis of the measured data. Since aluminum melt refinement takes 180 s in the operating conditions, the oxygen concentration value in water after 180 s of degasification was evaluated also in the case of physical modelling. However, the relevant values did not serve for derivation of hydrogen content in an aluminum melt in operating conditions; they served only for specification of trend dependencies of oxygen concentration in water on individual parameters and for designing of those variants which will be tested in low-pressure casting conditions.

**Figure 7** specifies quantitative efficiencies of individual variants for low-pressure casting according to the time of oxygen concentration decrease after 180 s of the degasification process. The graph distinguishes variants by color according to the speed (rpm) and, simultaneously, inside the columns it specifies the flow rate of argon defined for the relevant experiment. To provide a better overview, the variants were arranged according to the achieved oxygen concentrations after 180 s of the degasification process, from the lowest (the most efficient) to the highest (the least efficient). The graphs on **Figure 5** and **Figure 7** show clearly that with a few exceptions, after 180 s of the refinement process, lower oxygen concentrations were achieved at higher speed and higher argon flow rates. The lowest oxygen concentration in water, 1.64 ppm, achieved variant ① with the speed of 375 rpm and argon flow rate of 21  $\text{Nl}\cdot\text{min}^{-1}$ . On the other hand, variant ⑳ with 300 rpm and argon flow rate of 19  $\text{Nl}\cdot\text{min}^{-1}$  achieved the highest concentration of 4.72 ppm.

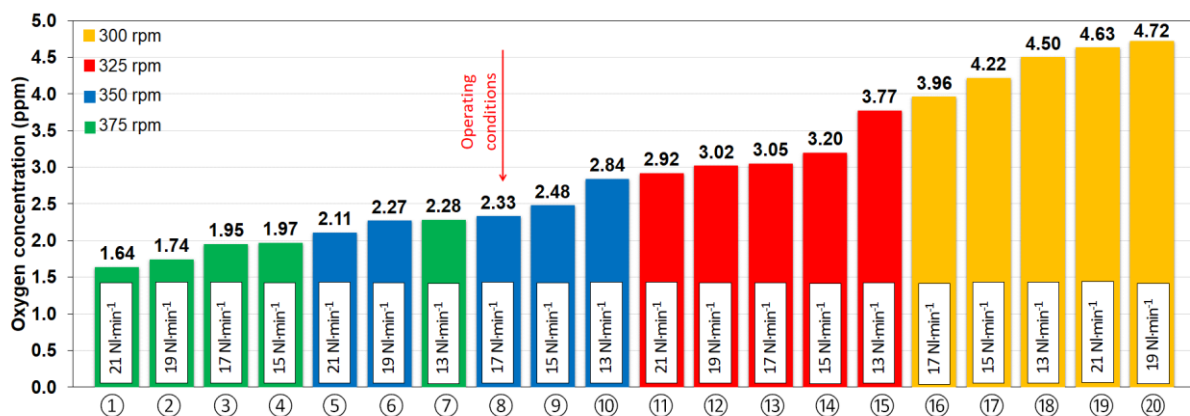


**Figure 7** Oxygen concentration in water after 180 s of the refinement process

Also the existing operation variant ⑧ with the parameters 350 rpm, 17  $\text{Nl}\cdot\text{min}^{-1}$  was modelled within the experiments. After 180 s, it achieved oxygen concentration of 2.33 ppm. **Figure 7** then shows that it would be possible to intensify the process by one operating parameter change. E.g., at maintaining the argon flow rate of 17  $\text{Nl}\cdot\text{min}^{-1}$  and speed increase to 375 rpm, after 180 s the oxygen concentration decreases to 1.95 ppm → variant ③. At maintaining the speed of 350 rpm and argon flow rate increase to 19  $\text{Nl}\cdot\text{min}^{-1}$  the achieved oxygen concentration dropped to 2.27 ppm → variant ⑥. The above specified shows clearly that the speed change has a more significant influence on the examined process than the argon flow rate change. This effect could have a positive influence in operating conditions as well. However, it is necessary to take into account also the negative impact of increased speed on the graphite components and on the process economy. Variants ③ and ⑥ will be further recommended for testing at operating conditions.

#### 4. CONCLUSIONS

This article deals with physical modelling of aluminum melt refinement on a FDU device, realized in laboratory conditions of the ITB in ČB. Crucial process parameters (speed, inert gas flow rate) have been selected in

cooperation with the operating partner; 20 variants tested on a physical model were selected on their basis. The experiments were realized with the use of a standard graphite rotor which serves in operating conditions. The following results can be specified on the basis of the physical modelling results:

- ✓ With increased speed and increased inert gas flow rate, the oxygen removal from water was faster in most of the variants. In case of variants with 375 rpm, after having achieved a certain oxygen concentration in water, ca 0.6 ppm, further concentration decrease slowed down significantly.
- ✓ Photographs were taken which document liquid flowing and the amount and distribution of argon bubbles in a ladle at various conditions setting.
- ✓ The operating variant ⑧ with 350 rpm and 17  $\text{Nl}\cdot\text{min}^{-1}$ , was tested within the modelling; after 180 s of degasification, it reached 2.33 ppm of oxygen in water.
- ✓ Other variants have been selected on the basis of the operating variant ⑧. Changing one process parameter achieved higher reduction of oxygen amount in water. Variant ③ worked with 375 rpm and argon flow rate of 17  $\text{Nl}\cdot\text{min}^{-1}$ . In case of this variant, after 180 s of degasification oxygen concentration achieved 1.95 ppm of oxygen. Next was variant ⑥ with 350 rpm and 19  $\text{Nl}\cdot\text{min}^{-1}$ , where after 180 s of degasification the oxygen concentration achieved 2.27 ppm.

In connection with the research related to physical modelling, operating tests will be carried out; their task will be to confirm the conclusions obtained through the physical model. The above mentioned variants ③ and ⑥ will be tested under operating conditions of low-pressure casting and, in case of good results, they will be implemented into standard technology applied in the MOTOR JIKOV Slévárna a.s.

## ACKNOWLEDGEMENTS

***The paper was prepared under the support of the Technology Agency of the Czech Republic within the scope of the EPSILON programme, as part of projects Reg. No. TH04010449 "Research and development of refining technologies for increasing of quality of aluminum alloys for high-performance quality castings".***

## REFERENCES

- [1] SIGWORTH, G. K., WILLIAMS E. M., CHESONIS D. C. Gas fluxing of molten aluminum: An overview. *Essential Readings in Light Metals*. 2013, pp. 65-70. Available from: <https://doi.org/10.1002/9781118647783.ch9>.
- [2] MICHNA, Š. et al. *Aluminium Materials and Technologies from A to Z*. Printed by Adin, s.r.o., Prešov, 2007.
- [3] Vesuvius. *FDU Foundry Degassing Unit* [online]. 2022 [viewed: 2022-5-5]. Available from: <https://www.vesuvius.com/content/dam/vesuvius/corporate/Our-solutions/our-solutions-master-english/foundry/non-ferrous-foundry/melt-treatment/brochures/FDU-e.pdf.downloadasset.pdf>.
- [4] SATERNUS, M., BOTOR J. Refining process of aluminum conducted in continuous Reactor - Physical model. *Archives of Metallurgy and Materials*. 2010, vol. 55, iss. 2, pp. 463-475.
- [5] SATERNUS M., MERDER T. Physical modelling of aluminum refining process conducted in batch reactor with rotary impeller. *Metals*. 2018, vol. 8, iss. 9, pp. 1-8. Available from: <https://doi.org/10.3390/met8090726>.
- [6] SATERNUS M., MERDER T. Physical modeling of the impeller construction impact on the aluminum refining process. *Materials*. 2022, vol. 15, iss. 2, pp. 1-11. Available from: <https://doi.org/10.3390/ma15020575>.
- [7] LICHÝ, P., BAJEROVÁ, M., KROUPOVÁ, I., OBZINA, T. Refining aluminum-alloy melts with graphite rotors. *Materiali in Technologije*. 2020, vol. 54, iss. 2, pp. 263–265. Available from: <https://doi.org/10.17222/mit.2019.147>.
- [8] MANCILLA, E., CRUZ-MÉNDEZ, W., RAMÍREZ-ARGÁEZ, M. A., GONZÁLEZ-RIVERA, C., ASCANIO, G. Experimental measurements of bubble size distributions in a aquatic model and its influence on the aluminum kinetics degassing. *The Canadian Journal of Chemical Engineering*. 2019, vol. 97, iss. S1, pp. 1729-1740. Available from: <https://doi.org/10.1002/cjce.23432>.

- [9] WU, J., DJAVANROODI, F., GODE, C., ATTARILAR, S., EBRAHIMI, M. Melt refining and purification processes in Al alloys: a comprehensive study. *Materials Research Express*. 2022, vol. 9, iss. 3. Available from: <https://doi.org/10.1088/2053-1591/ac5b03>.
- [10] ABREU-LÓPEZ, D., DUTTA, A., CAMACHO-MARTÍNEZ, J. L., TRÁPAGA-MARTÍNEZ, G., RAMÍREZ-ARGÁEZ, M.A. Mass transfer study of a batch aluminum degassing ladle with multiple designs of rotating impellers. *JOM*. 2018, vol. 70, iss. 12, pp. 2958-2967. Available from: <https://doi.org/10.1007/s11837-018-3147-y>.
- [11] CAMACHO-MARTÍNEZ, J. L., RAMÍREZ-ARGÁEZ, M.A., ZENIT-CAMACHO, R., JUÁREZ-HERNÁNDEZ, A., BARCEINAS-SÁNCHEZ, J.D.O., TRÁPAGA-MARTÍNEZ, G. Physical modelling of an aluminum degassing operation with rotating impellers. A comparative hydrodynamic analysis. *Materials and Manufacturing Processes*. 2010, vol. 25, iss. 7, pp. 581-591. Available from: <https://doi.org/10.1080/10426910903367386>.
- [12] CHEN, CH., WANG, J., SHU, D., XUE, J., SUN, B., XUE, Y., YAN, Q. Iron reduction in aluminum by electroslag refining. *Transactions of Nonferrous Metals Society of China*. 2012, vol. 22, iss. 4, pp. 964-969. Available from: [https://doi.org/10.1016/S1003-6326\(11\)61271-5](https://doi.org/10.1016/S1003-6326(11)61271-5).
- [13] WAN, H., XU, B., ZHAO, J., YANG, B., DAI, Y. *Analysis of the High-Purity Aluminum Purification Process Using Zone-Refining Technique*. Cham: Springer International Publishing, 2019, pp. 1697-1706. Available from: [https://doi.org/10.1007/978-3-030-05861-6\\_157](https://doi.org/10.1007/978-3-030-05861-6_157).
- [14] SOCHA, L., GRYC, K., SVIŽELOVÁ, J., PRÁŠIL, T., POSPÍŠIL, R., GRÁF, M. Assessment of rotary impeller efficiency by physical modelling of an aluminum refining process. In: *METAL 2021: 30th Anniversary International Conference on Metallurgy and Materials*. Ostrava: TANGER, 2021, pp. 1160-1165. Available from: <https://doi.org/10.37904/metal.2021.4258>.
- [15] SOCHA, L., GRYC, K., SVIŽELOVÁ, J., PRÁŠIL, T., POSPÍŠIL, R., GRÁF, M. Optimization of operating conditions of aluminum melt refining process in laboratory conditions. In: *METAL 2021: 30th Anniversary International Conference on Metallurgy and Materials*. Ostrava: TANGER, 2021, pp. 1166-1172. Available from: <https://doi.org/10.37904/metal.2021.4257>.